Title
Secreting and Sensing the Same Molecule Allows Cells to Achieve Versatile Social Behaviors

Journal
Science, 343(6171)

ISSN
0036-8075

Authors
Youk, Hyun
Lim, Wendell A

Publication Date
2014-02-07

DOI
10.1126/science.1242782

Peer reviewed

Published in final edited form as:
Science. 2014 February 7; 343(6171): 1242782. doi:10.1126/science.1242782.

Secreting and sensing the same molecule allows cells to achieve versatile social behaviors

Hyun Youk[1,2] and **Wendell A. Lim**[1,2,3,4]

[1]Department of Cellular and Molecular Pharmacology, University of California San Francisco, San Francisco, CA 94158, USA

[2]Center for Systems and Synthetic Biology, University of California San Francisco, San Francisco, CA 94158, USA

[3]Howard Hughes Medical Institute, University of California San Francisco, San Francisco, CA 94158, USA

Abstract

Cells that secrete and sense the same signaling molecule are ubiquitous. To uncover the functional capabilities of the core 'secrete-and-sense' circuit motif shared by these cells, we engineered yeast to secrete and sense the mating pheromone. Perturbing each circuit element revealed parameters that control the degree to which the cell communicated with itself versus with its neighbors. This tunable interplay of self- and neighbor-communication enables cells to span a diverse repertoire of cellular behaviors. These include a cell being asocial by responding only to itself, social through quorum sensing and an isogenic population of cells splitting into social and asocial subpopulations. A mathematical model explained these behaviors. The versatility of the secrete-and-sense circuit motif may explain its recurrence across species.

A central goal of systems biology is to understand how various cells use the common small repertoire of circuit elements to communicate with each other to achieve diverse functions (1-19). Of particular interest is the class of circuits that are found in cells that simultaneously secrete and sense the same extracellular molecule (Fig. 1A) because it is ubiquitous across species. Examples of such cells include (Fig. 1B) bacteria that secrete and sense the autoinducers for quorum-sensing (20-37), human pancreatic beta cells that secrete and sense insulin (38-39), vulva precursor cells in *C. elegans* that secrete and sense the diffusible Delta (40-44), and human T-cells that secrete and sense the cytokine interleukin-2 (IL-2) to regulate their growth (45-49). In some cases, a cell that secretes and senses the same molecule communicates with itself ('self-communication') but not with its neighboring cells, whereas in other cases such a cell communicates with its neighboring cells ('neighbor-communication') but not with itself. Moreover, in some cases, the secrete-and-sense cell communicates with both itself and with its neighbors (Fig. 1C). The advantages of using secrete-and-sense circuits have been unclear in many situations. For example, if a cell's primary purpose is self-communication, then it is unclear why the cell secretes a molecule instead of relying entirely on intracellular signaling. To address these questions, we

[4]To whom correspondence should be addressed: lim@cmp.ucsf.edu.

experimentally explored the full functional capabilities of the secrete-and-sense circuits that arise from the interaction between self- and neighbor-communication. We sought common design principles that tie together the seemingly disparate examples of secrete-and-sense circuits. We used the budding yeast's mating pathway as a model system in which we could systematically modify the secrete-and-sense circuits to determine what features affect the degree of self- vs. neighbor-communication. We demonstrate that varying the key parameters of the secrete-and-sense circuits allows cells to achieve diverse classes of behaviors, thus suggesting this class of circuits' functional flexibility may explain its recurrence throughout nature.

Results

Basic secrete-and-sense circuit in yeast

Our model ‘secrete-and-sense system’ is the haploid budding yeast that has been engineered to secrete and sense the mating pheromone, α–factor (50-60) (Fig. 1D). The cell senses the α–factor through its membrane receptor Ste2, and responds by expressing the green fluorescent protein (GFP) through the α–factor responsive promoter *pFUS1* (Fig. 1D, and fig. S1) (51). The cell increases GFP expression as the concentration of the exogenous α–factor increases. We used a *far1*Δ strain that did not arrest its cell cycle or mate upon stimulation by α-factor.

Disentangling effects of self-communication and neighbor-communication

To establish if the cell's response to sensing the molecule that it secreted (self-communication) could be distinguished from its response to the same molecule that had been secreted by its neighboring cells (neighbor-communication), we designed an experiment in which we cultured our secrete-and-sense strain with another strain, called the ‘sense-only’ strain, which senses but does not secrete α–factor (Fig. 2A). The sense-only strain could only respond to the α-factor secreted by the secrete-and-sense strain. On the other hand, a secrete-and-sense cell could potentially respond to both the α-factor that it secreted (self-communication) and the α-factor secreted by the other secrete-and-sense cells in the same batch liquid culture environment (neighbor-communication). Thus we reasoned that if we detected any difference between the reporter GFP levels of the secrete-and-sense strain (referred as ‘cell A’ throughout Fig. 2) and that of the sense-only strain (referred as ‘cell B’ throughout Fig. 2), then we could ascribe such effects to self-communication.

Construction of library of secrete-and-sense strains

We constructed a set of secrete-and-sense strains (Fig. 2B) and a set of sense-only strains (strain list in table S1). In each secrete-and-sense strain, doxycycline-inducible promoter *pTET07* expressed the *MFα1* gene that encodes α–factor (*MATa; bar1*Δ *far1*Δ) (Fig. 2B, and fig. S2). Doxycycline, a small molecule that readily diffused into the cell to control gene expression through the promoter *pTET07* was used to tune the secretion rate of the α–factor. Increasing concentration of doxycycline caused an increasing expression of the genes under the control of *pTET07*. The GFP expression was controlled by the promoter *pFUS1* that is induced by the α-factor (fig. S1) (51). We constructed various secrete-and-sense strains by varying the promoter that expressed Ste2. For each secrete-and-sense strain, we constructed

an analogous sense-only strain that lacked the *MFα1* gene. Each sense-only strain also constitutively expressed the fluorescent protein mCherry, which the secrete-and-sense strains lacked. This allowed us to use a flow cytometer to distinguish the sense-only strains from the secrete-and-sense strains when they were cultured together.

Experimental demonstration of self-communication

We cultured our 'basic secrete-and-sense strain' with its partner 'basic sense-only strain'. Both of these 'basic' strains had the same endogenous promoter *pSTE2* controlling expression of the Ste2 receptor (fig. S3). We grew these strains together at equal initial cell densities in 5mL of liquid medium in which we maintained a constant concentration of doxycycline. We used a flow cytometer to measure each strain's mean single-cell GFP fluorescence during the time-course. We cultured these strains at various total cell densities (ODs) and doxycycline concentrations (figs. S4-S7). When both the initial total cell density and the doxycycline concentration were low (e.g., OD = 0.001, [doxycycline]=6 μg/ml: Fig. 2C - left panel), the mean GFP fluorescence of the basic secrete-and-sense strain ('Cell A' in Fig. 2C - left panel) swiftly increased then plateaued whereas the mean GFP fluorescence of the basic sense-only strain ('Cell B' in Fig. 2C - left panel) stayed at a basal value throughout the time-course. This shows that each basic secrete-and-sense cell sensed and responded to the α–factor that it secreted whereas the amount of α–factor shared between cells (including between any two basic secrete-and-sense cells) was too low to activate the mating pathway. Thus each basic secrete-and-sense cell self-communicated in this regime of low cell density and secretion rate. In cultures with the same initial total cell density but with a higher doxycycline concentration (OD=0.001, [doxycycline]=30 μg/ml: Fig. 2C - right panel), the basic secrete-and-sense strain's GFP fluorescence again swiftly increased to a higher plateau than it did in the culture with the lower production of α–factor (i.e., compare 'Cell A' in both panels of Fig. 2C). GFP fluorescence of the basic sense-only strain also increased over time, albeit more slowly than that of the basic secrete-and-sense strain. Thus increasing the signal secretion rate increased the degree of neighbor-communication (including between different secrete-and-sense cells). The large discrepancy between the amounts of GFP fluorescence of the two strains indicates that each basic secrete-and-sense cell, in addition to communicating with its neighbors, also self-communicates by sensing and responding to the higher concentration of its own secreted α–factor. If there were no self-communication, both strains would have the same GFP fluorescence.

We examine cultures of the two basic strains at a 100-fold higher total cell density (OD=0.1 - Fig. 2D). In the high cell density co-culture with a low doxycycline concentration ([doxycycline]= 6 μg/ml: Fig. 2D - left panel), the basic sense-only strain's GFP fluorescence increased faster and to higher values than it did in the co-culture with the same doxycycline concentration but with the lower cell density (i.e., compared to 'cell B' in Fig. 2C - left panel). Thus the greater cell density caused the degree of neighbor-communication to increase. The change in cell density did not affect the basic secrete-and-sense strain's self-communication because the cell density does not affect its secretion rate of α–factor per cell, which is the main determinant of the degree of self-communication for the basic secrete-and-sense strain. In cultures with a high total cell density and a high secretion rate (OD=0.1, [doxycycline]= 30 μg/ml, Fig. 2D - right panel), there was virtually no difference in GFP

fluorescence between the two strains. Hence in these cultures, neighbor-communication was dominant.

Taken together, our co-culture experiments (Fig. 2, C and D) emphasize that self-communication and neighbor-communication, despite both using the same signaling molecule, do not always lead to the same behavior over time in a cell that secretes and senses the same molecule. In general, the dynamics of the cell's response to a signal depends not just on the type of the signaling molecule being sensed, but also on how the concentration of that molecule changes over time, and distinct dynamics of the same signaling pathway over time can lead to distinct cell fates (17). We developed a mathematical model that showed that the secrete-and-sense cell's response to self- and neighbor-communication yield distinct dynamical responses due to the fact that the two modes of communication involve different time scales (61). Our model also explains the main features of our culture experiments and quantifies the degree of self- and neighbor-communication (61).

High receptor expression and secretion rate enhance self-communication

We examined how varying the amount of the α-factor receptor, Ste2, affected the degrees of self-communication and of neighbor-communication. To do so, we repeated above experiments with strains that varied in the amount of Ste2 expressed (Fig. 2B, strains in table S1). In each pair, the secrete-and-sense and the sense-only strains used the same constitutive promoter to express Ste2 (figs. S8-S9). We cultured each pairs of strains as low cell density cultures (OD=0.001, Fig. 2E), as high cell density cultures (OD=0.1, Fig. 2F), and in a wide range of doxycycline concentrations. We used a flow cytometer to measure the mean single-cell GFP fluorescence of each strain after culturing each pair of strains for five hours in doxycycline together. By subtracting the mean single cell GFP fluorescence of the sense-only strain (‘Cell B’) from that of the secrete-and-sense strain (‘Cell A’), for each of the 7 pairs of strains in 11 different concentrations of doxycycline, we obtained ‘heat maps’ for low cell density (OD=0.001 for both strains: Fig. 2E) and high cell density (OD=0.1 for both strains: Fig. 2F) cultures. The color of each pixel in the heat maps (out of 7×11 pixels) represents the difference in the mean single cell GFP fluorescence of the two strains for each culture condition.

The heat map for low cell density (Fig. 2E) showed combinations of receptor abundance and secretion rate that enabled the secrete-and-sense cells to self-communicate, and those that did not allow for self-communication. Specifically, in the region of the heat map defined by high secretion rates ([doxycycline]>0.6 μg/ml) and high receptor expression values (top right quadrant of Fig. 2E), secrete-and-sense cells had higher GFP fluorescence than their counterpart sense-only cells whose GFP fluorescence remained near basal values (61). This indicates that a secrete-and-sense cell with a high secretion rate and a high receptor expression is ‘asocial’ cell that self-communicates by efficiently capturing its own α-factor due to its highly abundant receptors. The secrete-and-sense cells with high secretion rates ([doxycycline] > 0.6 μg/ml) and lower range of receptor expression values (lower right quadrant of the heat map in Fig. 2E) had nearly the same GFP fluorescence values as their counterpart sense-only cells. This indicates that a secrete-and-sense cell with a low receptor

expression and high secretion rate is a 'social' cell that is unable self-communicate because its receptor abundance is too low to capture its own α–factor for activating its mating pathway, but is ideal for communicating with its neighbors due to its high secretion rate (61). The secrete-and-sense cells with low secretion rate ([doxycycline] < 0.6 μg/ml: the left half of heat map in Fig. 2E), including those with high receptor abundances, had nearly same GFP fluorescence as their counterpart sense-only cells. This indicates that these secrete-and-sense cells cannot self-communicate because they do not secrete enough α-factor, leading to negligible self and neighbor communication in low cell density. The heat map for high cell density (Fig. 2F) showed that secrete-and-sense cells and sense-only cells had nearly identical GFP fluorescence at all secretion rate and receptor expression values. This indicates that increasing the density of secrete-and-sense cells increases the neighbor-communication due to the increased total population-level secretion of α-factor.

Positive feedback on self- and neighbor-communication enables binary cell fates

We next examined how the secrete-and-sense cell's degree of sociability could be further modulated by two regulatory mechanisms that are ubiquitous in naturally occurring secrete-and-sense circuits: Positive feedback link (detection of the molecule leads to increased secretion of the molecule) (62-64) and active degradation of the signaling molecule (e.g., secretion of a protease) (20).

We first investigated the influence of self- and neighbor-communication on the positive feedback link. To the basic secrete-and-sense circuit (used in Fig. 2, B and C), we added a positive feedback link (highlighted in blue, Fig. 3A) in which production of α-factor was induced by the mating pathway by linking the *rtTA* expression by the promoter *pFUS1* and having the promoter *pTET07* expressing *MFα1*. We engineered this synthetic positive feedback link so that its strength could be tuned by increasing the doxycycline concentration (fig. S10). We cultured this positive feedback equipped secrete-and-sense strain by itself in a wide range of doxycycline concentrations and at various cell densities. For each condition, we used a flow cytometer to obtain the histograms of mean single-cell GFP fluorescence at various time points (Fig. 3, B and C, figs. S11 and S12). When the cell density was low (OD=0.001) and the positive feedback was weak (e.g., [doxycycline]= 3 μg/ml), this strain's GFP fluorescence remained at basal values throughout the time-course (Fig. 3B - left column). This corresponds to an 'OFF-state' in which the cell secretes the α-factor at a low basal rate (indicated by its low basal GFP fluorescence). When positive feedback was strong in cultures of low cell density (e.g., [doxycycline] = 40 μg/ml, Fig. 3B - right column) cells, which were initially in the OFF-state, increased their signal response over time (corresponding to increasing its signal secretion rate) and after 8 hours, reached a maximally allowed response - the 'ON-state' - in which cells secreted α-factor at the maximal possible rate (Fig. 3B - right column and fig. S11). Thus positive feedback enabled the initially quiescent secrete-and-sense cell to be 'activated' to become maximally secreting cells. This behavior occurs in many natural secrete-and-sense cells with a similar positive feedback link (e.g., cytokine signaling in T-cells) (47, 48, 62, 63, 65-68).

At a high cell density (OD=0.1), if the positive feedback was weak (e.g., [doxycycline] = 3 μg/ml, Fig. 3C - left column) the cells activated whereas they remained in the OFF-state in

cultures of lower cell density with the same doxycycline concentration (Fig. 3B - left column) (fig. S12). This indicates that increased neighbor-communication, through the population's collective amplification of the basal level secretion from each cell, probably accounts for this activation (Fig. 3C - left column).

To address whether these activation properties were due to self-communication or neighbor-communication, we incubated the positive feedback-equipped basic secrete-and-sense strain (Fig. 3A) with the analogous sense-only strain (characterized in fig. S10) under various doxycycline and cell density conditions (fig. S13). At low total cell density (OD=0.001), the sense-only strain's GFP fluorescence remained at the basal values during the activation of the secrete-and-sense strain at all doxycycline concentrations. Thus self-communication, through a cell's small rate of basal secretion, accounts for the ‘self-activation’ at this low cell density (fig. S13). At a high total cell density (OD=0.1), the sense-only strain's GFP signal increased at the same time as the secrete-and-sense cells were being activated, indicating that neighbor-communication caused the activation (fig. S13). Thus at sufficiently high density, secrete-and-sense cells with positive feedback collectively amplify each cell's basal secretion of α-factor, leading to a ‘neighbor-activation’.

To summarize, self-activation can occur without any neighbor-communication whereas neighbor-activation can occur in regimes where self-communication is insufficient for self-activation of the secrete-and-sense cells with the positive feedback link. Neighbor-communication strengthens the positive feedback, enabling even a very weak positive feedback secrete-and-sense circuit to behave as if it had a strong positive feedback. Self-communication, through sufficiently strong positive feedback, enables the secrete-and-sense cells with a very low secretion rate to self-activate so that they can communicate with their neighbors. The interplay between self- and neighbor-communication creates the overall population level behavior, in which all cells activate in near unison (Fig. 3D) (61). Our work shows that understanding this collective behavior of the secrete-and-sense circuit with the positive feedback link requires knowing the properties of both the intracellular circuit and the communication between the secrete-and-sense cells.

Signal degradation with positive feedback enables bimodal cellular differentiation

We also examined the effects of an active signal-degradation mechanism in secrete-and-sense circuits. We engineered our positive feedback-equipped basic secrete-and-sense strain to express the Bar1 protease (50, 52-54), which degrades α-factor in the periplasmic space of the yeast cell (Fig. 4A). We constructed a set of such strains, each with a different constitutive promoter that controls the Bar1 expression (strength of promoters shown in fig. S8, figs. S14 and S15).

A strain that had a weak constitutive expression level of Bar1 (Fig. 4, B and C, fig. S15) was incubated by itself at low (OD=0.001) or high (OD=0.1) cell density and in various concentrations of doxycycline. When its positive feedback was weak (e.g., [doxycycline] = 6 μg/ml), the strain remained in the OFF-state in the low cell density culture (Fig. 4B - left column) and was activated at high cell density (Fig. 4C - left column). Increasing expression of Bar1 decreased the rate at which activation occurred (fig. S15). When positive feedback was sufficiently strong (e.g., [doxycycline]=20 μg/ml), for the low (Fig. 4B -right column)

and high (Fig. 4C - right column) cell densities, a transient mixture of OFF-state and ON-state cells was observed in the isogenic culture. In this bimodal population, consisting of isogenic cells that were all initially in the OFF-state, all the cells in the OFF-state were eventually activated to the ON-state (fig. S15). At high cell density (OD=0.1), the cells were activated faster (Fig. 4C - right column), consistent with our finding that increasing the degree of neighbor-communication increased the rate at which the secrete-and-sense cells could be activated.

By examining the individual time-courses for all our strains with Bar1 expression (fig. S14 and S15), we obtained a phase diagram that summarizes how the population level behaviors depend on the positive feedback strength and the Bar1 abundance (Fig. 4D). From our mathematical model (61) we obtained an intuitive explanation of this phase diagram. When the cells express very high amounts of Bar1, no activation (self or neighbor) can occur because the high activity of Bar1 degrades the basally secreted α-factor produced by each cell. When the cell density is low, the secrete-and-sense cells rely on self-communication for their activation. If in the low cell density cultures, the secrete-and-sense cells express a low amount of Bar1 and use a strong positive feedback link, then they will self-activate in a digital (ON or OFF) manner, which manifests as a bimodal population of quiescent and maximally secreting cells (Fig. 4E). This results from cell-to-cell variability in the threshold for activation (i.e., the amount of α–factor required for activation). At a sufficiently high cell density, neighbor-activation dominates and because every cell essentially senses the same concentrations of α–factors produced by collective basal secretion, the bimodal activation can disappear (as cell-to-cell variability becomes less relevant) and cells can activate together in a graded fashion (61). Without the positive feedback, signal degradation's role is weakening the secreted signal. But when coupled with positive feedback, signal degradation has important effects on the population level behaviors of secrete-and-sense circuits that reach beyond just weakening of the secreted signal. This may suggest why signal degradation mechanisms are often present in conjunction with positive feedback links in naturally occurring secrete-and-sense circuits. Bar1, coupled with positive feedback, enables a secrete-and-sense cell to delay its response to signal and a population to ‘hedge its bets’ by responding in two distinct ways (i.e., bimodal activation, Fig. 4E) by tuning the threshold for activation. Moreover, cells can suppress self-activation while only allowing neighbor-activation.

Intuitive phenomenological model

We developed a simple mathematical model that ties together various roles of self- and neighbor-communication (61). Its central idea is that self-communication competes with neighbor-communication since they both use the same molecule and receptor. A secrete-and-sense cell can build a locally high concentration of α-factor that it secreted. In low cell densities, this occurs faster than the rate at which the concentration far from the secrete-and-sense cell (the ‘global concentration’) changes. Sensing of the locally high α–factor concentration leads to the fast increases in the secrete-and-sense cell's response (‘self-communication’ in Fig. 5A, and fig. S16) whereas the slowly changing global concentration of the α-factor leads to a slow response in sense-only cells at low cell density (‘neighbor-communication’ in Fig. 5A, and figs. S17-S19) (61). Paradoxically, self-communication in

effect insulates a secrete-and-sense cell from responding to the α–factor that is secreted by the other secrete-and-sense cells. Our model quantifies and summarizes the degree of self- and neighbor-communication in a phase diagram these key features (Fig. 5B) (61). It also aids in understanding the competition between the positive feedback and the effects of the active signal degradation (figs. S20-S23) (61). Our simple model thus provides an intuitive explanation of the main principles underlying the results our experiments.

Discussion

Translating knowledge from synthetic to natural systems

By integrating simple mathematical models, measurements on single cells and whole populations, and a bottom-up synthetic biology approach, we revealed a diverse repertoire of biological functions that secrete-and-sense cells can achieve. Crucially, this integrated approach uncovered design principles that enable the circuit to tune the balance between self- and neighbor-communication among cells – a crucial mechanism for achieving myriad cellular behaviors and an important general issue in biology. Our work provides a framework for designing synthetic secrete-and-sense circuits and better understanding the diverse behaviors of seemingly disparate natural secrete-and-sense cells (Table 1). For example, bacterial quorum sensing - a purely ‘social’ behavior (Fig. 5C) - relies on the low secretion rate of an autoinducer and the low expression level of a low-affinity receptor to prohibit self-communication and allow only neighbor-communication (27, 31, 33, 69). Epithelial cells predominantly self-communicate through a signaling loop, commonly referred to as ‘autocrine signaling loop’ (38-49, 70-74), by expressing large amount of EGF-receptor and secreting epidermal growth factor (EGF), which the receptor recognizes, at sufficiently high rates (73) - a purely ‘asocial’ behavior (Fig. 5C).

‘Self-activation’ (Fig. 5C) occurs in T helper (Th) cells when they use positive feedback on the cytokine interleukin-2 (IL-2) that they secrete and sense to sharply increase their proliferation rate in a switch-like fashion. Specifically, Th cells increase both the expression of high-affinity IL-2 receptor and secretion rate of IL-2, which enhances their self-communication through IL-2 that enables them to turn on their proliferation switch. This promotes a monoclonal expansion of cells within an initially polyclonal population of T-cells, despite the fact that all cells in the population have the same underlying network for processing IL-2 signal (45-48, 62).

Importantly, aside from known cellular behaviors, our work suggests that simultaneous self- and neighbor-communication may be a crucial mechanism to consider for interpreting behaviors of secrete-and-sense cells that are currently poorly understood. In particularly, there are numerous examples of poorly understood cytokine-mediated decisions in immunology and developmental biology. For example, recent studies have revealed that naive Th cells can realize a tunable hybrid of the two Th cell states: Th1 and Th2, which is controlled by secreting and sensing cytokines interferon-γ and interleukin-4 (75, 76). Self- and neighbor-communication through these cytokines have both been implicated as the main factors that determine the distribution of the hybrid cell fates in the population but the details are unknown. Our work suggests that the simultaneous self- and neighbor-communication in these T cells may be understood by measuring the cell density and individual T cell's

receptor expression and secretion rate through single-cell measurement techniques. In the cells of developing embryos, secreting and sensing hedgehog signaling molecules such as the Sonic Hedgehog (Shh) are crucial for cell fate specification, including in the embryos of fruit flies, mice, and humans (77). Although it is known that these cells use combinations of autocrine and paracrine signaling of hedgehog signaling molecules for proper cell-fate specification, the difference in the dynamics of individual cells' response to the same signaling molecule determined by self- and neighbor-communication has not received much attention. Insights provided by recent studies on quantitative single-cell dynamics in developing embryos indicate that the different time scales of individual cell's response, such as those that would be generated by self- and neighbor-communication through the same molecule, is central for a reliable and timely developmental patterning that is reproducible between individuals (78-83). This is especially true in spatially organized cells – an important scenario that our work did not address. Our work suggests that in addition to identifying the signaling pathways, the approaches we use to distinguish whether a pathway is self- or neighbor-activated is crucial to understand developmental process of animals.

In engineering secrete-and-sense cells, our work shows that it is possible to design microbes that can achieve ‘diffusion sensing’ (84), a hypothetical mechanism for self-communication in bacteria akin to mammalian autocrine signaling (70), which was proposed but lacked a clear demonstration. Our work suggests that by increasing the receptor expression of bacteria that sense a quorum, they can be converted to diffuse-sense, which may be useful in bio-production applications. Such cells may integrate self-and quorum-sensing to make sophisticated and autonomous decisions about optimal switching times between growth and bio-fuel production phases. Indeed some of the yeast strains engineered in our study may be useful for large scale bio-fermentation, in which adding external inducer molecules is prohibitively expensive. Moreover, the ability to tune self- vs. neighbor-communication in multicellular microbial systems, such as the social amoebae *Dictyostelium discoideum* or biofilms, may provide a way to better understand the advantages of cooperative vs. self-driven behaviors (20-25, 85, 86).

Evolution appears to favor efficient circuits and signaling elements that can accomplish many different tasks (13, 14). The diverse social behaviors that are enabled by the functional flexibility of the secrete-and-sense circuits (Fig. 5C) may explain the frequent occurrence of this class of circuits' in nature.

Dissecting multicellular behaviors through bottom-up synthetic biology approach

Beyond understanding secrete-and-sense circuits, our approach may be generalized to reveal how cells use fundamental cell signaling circuits to achieve complex multicellular behaviors. Synthetic cell-signaling circuits, including some capable of quorum sensing, have often been used to demonstrate targeted cellular behaviors and engineering goals (e.g., cellular logic gates) (3, 28, 33, 34, 37, 87-94). Our work highlights alternate use of synthetic circuits - For exploring their full capabilities and understanding them in a framework that unites natural and synthetic systems that share the same circuit motif (95-97). While only a handful of canonical signaling pathways and circuit motifs are repeatedly used across species, how they produce multicellular organisms and their behaviors is poorly understood

at a systems-level (98). By building synthetic signaling circuits that mimic the natural signaling circuits, one can perturb each circuit element in individual cells, measure its effects on intracellular and intercellular interactions, and then bridge these interactions to the whole population level behavior. Doing so may help us understand how the myriad interactions from molecules to cells are coordinated to yield higher-order complex multicellular behaviors (2).

Supplementary Material

Refer to Web version on PubMed Central for supplementary material.

Acknowledgments

We thank A. Mitchell, S. Itzkovitz, T. Long, M. Thomson, E. Puchner, K. Roybal, L. Morsut, D. Sivak, A. Raj, and J. Gore for insightful discussions. This work was supported by NIH grants R01 GM55040, R01 GM62583, PN2 EY016546, P50 6M081879 (to W.A.L.), and the Howard Hughes Medical Institute (to W.A.L.). H.Y. is a HHMI Fellow of the Damon Runyon Cancer Research Foundation (DRG-2089-11).

References and Notes

1. Afek Y, et al. A biological solution to a fundamental distributed computing problem. Science. 2011; 331:183–185. [PubMed: 21233379]
2. Mehta P, Gregor T. Approaching the molecular origins of collective dynamics in oscillating cell populations. Curr Opinion Genet & Dev. 2010; 20:574–580.
3. Mondragon-Palomino O, Danino T, Selimkhanov J, Tsimring L, Hasty J. Entrainment of a population of synthetic genetic oscillators. Science. 2011; 333:1315–1319. [PubMed: 21885786]
4. Sprinzak D, et al. Cis-interactions between notch and delta generate mutually exclusive signaling states. Nature. 2010; 465:86. [PubMed: 20418862]
5. von Dassow G, Meir E, Munro EM, Odell GM. The segment polarity network is a robust developmental module. Nature. 2000; 406:188–192. [PubMed: 10910359]
6. Wong JV, Li B, You L. Tension and robustness in multitasking cellular networks. PLoS Comp Biol. 2012; 8:e1002491.
7. de Ronde WH, Tostevin F, ten Wolde PR. Multiplexing biochemical signals. Phys Rev Lett. 2011; 107:048101. [PubMed: 21867046]
8. Hermsen R, Ursem B, ten Wolde PR. Combinatorial gene regulation using auto-regulation. PLoS Comp Biol. 2010; 6:e1000813.
9. Chen JY, Lin JR, Cimprich KA, Meyer T. A two-dimensional ERK-AKT signaling code for an NGF-triggered cell-fate decision. Mol Cell. 2012; 45:196–209. [PubMed: 22206868]
10. Bollenbach T, Kishony R. Resolution of gene regulatory conflicts caused by combinations of antibiotics. Mol Cell. 2011; 42:413–425. [PubMed: 21596308]
11. Espinar L, Dies M, Cagatay T, Suel GM, Garcia-Ojalvo J. Circuit-level input integration in bacterial gene regulation. Proc Natl Acad Sci U S A. 2013; 110:7091–7096. [PubMed: 23572583]
12. Hart Y, Alon U. The utility of paradoxical components in biological circuits. Mol Cell. 2013; 49:213. [PubMed: 23352242]
13. Shen-Orr S, Milo R, Mangan S, Alon U. Network motifs in the transcriptional regulation network of Escherichia coli. Nat Genet. 2002; 31:64–68. [PubMed: 11967538]
14. Milo R, et al. Network motifs: Simple building blocks of complex networks. Science. 2002; 298:824–827. [PubMed: 12399590]
15. Gao J, Buldyrev SV, Stanley HE, Havlin S. Networks formed from interdependent networks. Nat Phys. 2012; 8:40–48.
16. Davidson EH. Emerging properties of animal gene regulatory networks. Nature. 2010; 468:911–920. [PubMed: 21164479]

17. Purvis JE, Lahav G. Encoding and decoding cellular information through signaling dynamics. Cell. 2013; 152:945. [PubMed: 23452846]
18. Tegner J, Yeung MKS, Hasty J, Collins JJ. Reverse engineering gene networks: Integrating genetic perturbations with dynamical modeling. Proc Natl Acad Sci U S A. 2003; 100:5944. [PubMed: 12730377]
19. Ferrell JE Jr, et al. Simple, realistic models of complex biological processes: positive feedback and bistability in a cell fate switch and a cell cycle oscillator. FEBS Lett. 2009; 583:3999. [PubMed: 19878681]
20. Gregor T, Fujimoto K, Masaki N, Sawai S. The onset of collective behavior in social amoebae. Science. 2010; 328:1021–1025. [PubMed: 20413456]
21. De Monte S, d'Ovidio F, Dano S, Graae Sorensen P. Dynamical quorum sensing: Population density encoded in cellular dynamics. Proc Natl Acad Sci U S A. 2007; 104:18377–18381. [PubMed: 18003917]
22. Schwab DJ, Baetica A, Mehta P. Dynamical quorum-sensing in oscillators coupled through an external medium. Physica D. 2012; 241:1782–1788. [PubMed: 23087494]
23. Sawai S, Thomason PA, Cox EC. An autoregulatory circuit for long-range self-organization in Dictyostelium cell populations. Nature. 2005; 433:323–326. [PubMed: 15662425]
24. Li L, Cox EC, Flyvbjerg H. 'Dicty dynamics': Dictyostelium motility as persistent random motion. Phys Biol. 2011; 8:046006. [PubMed: 21610290]
25. Umeda T, Inouye K. Cell sorting by differential cell motility: a model for pattern formation in Dictyostelium. J Theor Biol. 2004; 226:215–224. [PubMed: 14643191]
26. Ng WL, Bassler BL. Bacterial quorum-sensing network architectures. Annu Rev of Genet. 2009; 43:197–222. [PubMed: 19686078]
27. Tu KC, Long T, Svenningsen SL, Wingreen NS, Bassler BL. Negative feedback loops involving small regulatory RNAs precisely control the Vibrio harveyi quorum-sensing response.
28. You L, Cox RS, Weiss R, Arnold FH. Programmed population control by cell-cell communication and regulated killing. Nature. 2004; 428:868–871. [PubMed: 15064770]
29. Bischofs IB, Hug JA, Liu AW, Wolf DM, Arkin AP. Complexity in bacterial cell-cell communication: quorum signal integration and subpopulation signaling in the Bacillus subtilis phosphorelay. Proc Natl Acad Sci U S A. 2009; 106:6459–6464. [PubMed: 19380751]
30. Mehta P, Goyal S, Long T, Bassler BL, Wingreen NS. Information processing and signal integration in bacteria quorum sensing. Mol Sys Biol. 2009; 5:325.
31. Eldar A. Social conflict drives the evolutionary divergence of quorum sensing. Proc Natl Acad Sci U S A. 2011; 108:13635–13640. [PubMed: 21807995]
32. Pai A, Tanouchi Y, You L. Optimality and robustness in quorum sensing (QS)-mediated regulation of a costly public good enzyme. Proc Natl Acad Sci U S A. 2012; 109:19810. [PubMed: 23144221]
33. Williams TC, Nielsen LK, Vickers CE. Engineered quorum sensing using pheromone-mediated cell-to-cell communication in Saccharomyces cerevisiae. ACS Synth Biol. 2013; 2:136–149. [PubMed: 23656437]
34. Danino T, Mondragon-Palomino O, Tsimring L, Hasty J. A synchronized quorum of genetic clocks. Nature. 2010; 463:326–330. [PubMed: 20090747]
35. Teng S, et al. Active regulation of receptor ratios controls integration of quorum-sensing signals in Vibrio harveyi. Mol Sys Biol. 2011; 7:491.
36. Chatterjee A, et al. Antagonistic self-sensing and mate-sensing signaling controls antibiotic-resistance transfer. Proc Natl Acad Sci U S A. 2013; 110:7086–7090. [PubMed: 23569272]
37. Chen MT, Weiss R. Artificial cell-cell communication in yeast Saccharomyces cerevisiae using signaling elements from Arabidopsis thaliana. Nat Biotech. 2005; 23:1551–1555.
38. Leibiger IB, Leibiger B, Berggren PO. Insulin signaling in the pancreatic β-cell. Annu Rev Nutr. 2008; 28:233–251. [PubMed: 18481923]
39. Aspinwall CA, Lakey JRT, Kennedy RT. Insulin-stimulated insulin secretion in single pancreatic beta cells. J Biol Chem. 1999; 274:6360–6365. [PubMed: 10037726]

40. Hoyos E, et al. Quantitative variation in autocrine signaling and pathway crosstalk in the *Caenorhabditis* vulval network. Curr Biol. 2011; 21:527–538. [PubMed: 21458263]
41. Chen N, Greenwald I. The lateral signal for LIN-12/Notch in *C. elegans* vulval development comprises redundant secreted and transmembrane DSL proteins. Dev Cell. 2004; 6:183–192. [PubMed: 14960273]
42. Seydoux G, Greenwald I. Cell autonomy of lin-12 function in a cell fate decision in *C. elegans*. Cell. 1989; 57:1237–1245. [PubMed: 2736627]
43. Sternberg PW, Horvitz HR. The combined action of two intercellular signaling pathways specifies three cell fates during vulval induction in *C. elegans*. Cell. 1989; 58:679–693. [PubMed: 2548732]
44. Corson F, Siggia ED. Geometry, epistasis, and developmental patterning. Proc Natl Acad Sci U S A. 2012; 109:5568–5575. [PubMed: 22434912]
45. Cantrell DA, Smith KA. The interleukin-2 T-cell system: a new cell growth model. Science. 1984; 224:1312–1316. [PubMed: 6427923]
46. Waldmann TA. The biology of interleukin-2 and interleukin-15: Implications for cancer therapy and vaccine design. Nat Rev Immunol. 2006; 6:595–601. [PubMed: 16868550]
47. Savir Y, Waysbort N, Antebi YE, Tlusty T, Friedman N. Balancing speed and accuracy of polyclonal T cell activation: a role for extracellular feedback. BMC Sys Biol. 2012; 6:111.
48. Feinerman O, et al. Single-cell quantification of IL-2 response by effector and regulatory T cells reveals critical plasticity in immune response. Mol Sys Biol. 2010; 6:437.
49. Fallon EM, Lauffenburger DA. Computational model for effects of ligand/receptor binding properties on interleukin-2 trafficking dynamics and T cell proliferation response. Biotechnol Prog. 2000; 16:905–916. [PubMed: 11027188]
50. Bardwell L. A walk-through of the yeast mating pheromone responsive pathway. Peptides. 2004; 25:1465–1476. [PubMed: 15374648]
51. Bashor CJ, Helman NC, Yan S, Lim WA. Using engineered scafold interactions to reshape MAP kinase pathway signaling dynamics. Science. 2008; 319:1539–1543. [PubMed: 18339942]
52. Barkai N, Rose M, Wingreen N. Protease helps yeast find mating partners. Nature. 1998; 396:422–423. [PubMed: 9853747]
53. Rappaport N, Barkai N. Disentangling signaling gradients generated by equivalent sources. J Biol Phys. 2012; 38:267–278. [PubMed: 23450187]
54. Jin M, et al. Yeast dynamically modify their environment to achieve better mating efficiency. Sci Signal. 2011; 4:ra54. [PubMed: 21868361]
55. Goncalves-Sa J, Murray A. Asymmetry in sexual pheromones is not required for ascomycete mating. Curr Biol. 2011; 21:1337–1346. [PubMed: 21835624]
56. Hao N, et al. Regulation of cell signaling dynamics by the protein kinase-scaffold Ste5. Molec Cell. 2008; 30:649–656. [PubMed: 18538663]
57. Ingolia NT, Murray AW. Positive-feedback loops as a flexible biological module. Curr Biol. 2007; 17:668–677. [PubMed: 17398098]
58. Yu RC, et al. Negative feedback that improves information transmission in yeast signalling. Nature. 2008; 456:755–761. [PubMed: 19079053]
59. Madhani, HD. From a to alpha: Yeast as a model for cellular differentiation. Cold Spring Harbor Laboratory Press; 2006.
60. McCullagh E, Seshan A, El-Samad H, Madhani HD. Coordinate control of gene expression noise and interchromosomal interactions in a MAP kinase pathway. Nat Cell Biol. 2010; 12:954–962. [PubMed: 20852627]
61. Full details are available as Supplementary Materials on *Science* Online.
62. Hart Y, Antebi YE, Mayo AE, Friedman N, Alon U. Design principles of cell circuits with paradoxical components. Proc Natl Acad Sci U S A. 2012; 109:8346–8351. [PubMed: 22562798]
63. Ferrell JE Jr. Feedback regulation of opposing enzymes generates robust, all or none bistable responses. Curr Biol. 2008; 18:R244–245. [PubMed: 18364225]
64. Hornung G, Barkai N. Noise propagation and signaling sensitivity in biological networks: a role for positive feedback. PLoS Comp Biol. 2008; 4:e8.

65. Hasty J, Pradines J, Dolnik M, Collins JJ. Noise-based switches and amplifiers for gene expression. Proc Natl Acad Sci U S A. 2000; 97:2075–2080. [PubMed: 10681449]
66. Hermsen R, Erickson D, Hwa T. Speed, sensitivity, and bistability in auto-activating signaling circuits. PLoS Comp Biol. 2011; 7:e1002265.
67. Feinerman O, Veiga J, Dorfman JR, Germain RN, Altan-Bonnet G. Variability and robustness in T cell activation from regulated heterogeneity in protein levels. Science. 2008; 321:1081–1084. [PubMed: 18719282]
68. Sansone P, et al. IL-6 triggers malignant features in mammospheres from human ductal breast carcinoma and normal mammary gland. J Clin Invest. 2007; 117:3988–4002. [PubMed: 18060036]
69. Long T, et al. Quantifying the integration of quorum-sensing signals with single-cell resolution. PLoS Biol. 2009; 7:e68. [PubMed: 19320539]
70. Sporn MB, Todaro GJ. Autocrine secretion and malignant transformation of cells. N Engl J Med. 1980; 303:878–880. [PubMed: 7412807]
71. Coppey M, Berezhovskii AM, Sealfon SC, Shvartsman SY. Time and length scales of autocrine signals in three dimensions. Biophysical Journal. 2007; 93:1917–1922. [PubMed: 17720734]
72. Shvartsman SY, Wiley HS, Deen WM, Lauffenburger DA. Spatial range of autocrine signaling: modeling and computational analysis. Biophys J. 2001; 81:1854–1867. [PubMed: 11566760]
73. DeWitt AE, Dong JY, Wiley HS, Lauffenburger DA. Quantitative analysis of the EGF receptor autocrine system reveals cryptic regulation of cell response by ligand capture. J Cell Sci. 2001; 114:2301–2313. [PubMed: 11493669]
74. Shvartsman SY, et al. Autocrine loops with positive feedback enable context-dependent cell signaling. Am J Physiol Cell Physiol. 2002; 282:C545–559. [PubMed: 11832340]
75. Antebi YE, et al. Mapping differentiation under mixed culture conditions reveals a tunable continuum of T cell fates. PLoS Biol. 2013; 11:e1001616. [PubMed: 23935451]
76. Fang M, Xie H, Dougan SK, Ploegh H, van Oudenaarden A. Stochastic cytokine expression induces mixed T helper cell states. PLoS Biol. 2013; 11:e1001618. [PubMed: 23935453]
77. Lum L, Beachy PA. The hedgehog response network: Sensors, switches, and routers. Science. 2004; 304:1755–1759. [PubMed: 15205520]
78. Gregor T, Wieschaus EF, Tank DW, Bialek W. Probing the limits to positional information. Cell. 2007; 130:153–164. [PubMed: 17632062]
79. Liu F, Morrison AH, Gregor T. Dynamic interpretation of maternal inputs by the Drosophila segmentation gene network. Proc Natl Acad Sci U S A. 2013; 110:6724–6729. [PubMed: 23580621]
80. Garcia HG, Tikhonov M, Lin A, Gregor T. Quantitative imaging of transcription in living Drosophila embryos links polymerase activity to patterning. Curr Biol. 2013; 23:2140–2145. [PubMed: 24139738]
81. Dubuis JO, Samanta R, Gregor T. Accurate measurements of dynamics and reproducibility in small genetic networks. Mol Sys Biol. 2012; 9:639.
82. Haskel-Ittah M, et al. Self-organized shuttling: Generating sharp dorsoventral polarity in the early drosophila embryo. Cell. 2012; 150:1016–1028. [PubMed: 22939625]
83. Ben-Zvi D, Shilo BZ, Fainsod A, Barkai N. Scaling of the BMP activation gradient in Xenopus embryos. Nature. 2008; 453:1205–1211. [PubMed: 18580943]
84. Redfield R. Is quorum sensing a side effect of diffusion sensing? Trends in Microbiol. 2002; 10:365–370.
85. Brock DA, Douglas TE, Queller DC, Strassmann JE. Primitive agriculture in a social amoeba. Nature. 2011; 469:393–396. [PubMed: 21248849]
86. Gore J, Youk H, van Oudenaarden A. Snowdrift game dynamics and facultative cheating in yeast. Nature. 2009; 459:253–256. [PubMed: 19349960]
87. Basu S, Gerchman Y, Collins CH, Arnold FH, Weiss R. A synthetic multicellular system for programmed pattern formation. Nature. 2005; 434:1130–1134. [PubMed: 15858574]
88. Tabor JJ, et al. A synthetic genetic edge detection program. Cell. 2009; 137:272–1281.
89. Balagadde FK, et al. A synthetic Escherichia coli predator-prey ecosystem. Mol Syst Biol. 2008; 4:1–8.

90. Tasmir A, Tabor JJ, Voigt CA. Robust multicellular computing using genetically encoded NOR gates and chemical 'wires'. Nature. 2011; 469:212–215. [PubMed: 21150903]

91. Regot S, et al. Distributed biological computation with multicellular engineered networks. Nature. 2011; 469:207–211. [PubMed: 21150900]

92. Galloway KE, Franco E, Smolke CD. Dynamically reshaping signaling networks to program cell fate via genetic controllers. Science. 2013; 341:1358.

93. Bonnet J, Yin P, Ortiz ME, Subsoontorn P, Endy D. Amplifying genetic logic gates. Science. 2013; 340:599–603. [PubMed: 23539178]

94. Liu C, et al. Sequential establishment of stripe patterns in an expanding cell population. Science. 2011; 334:238–241. [PubMed: 21998392]

95. Elowitz MB, Lim WA. Build life to understand it. Nature. 2010; 468:889–890. [PubMed: 21164460]

96. Velenich A, Gore J. Synthetic approaches to understanding biological constraints. Curr Opinion in Chemical Biol. 2012; 16:323–328.

97. Chen S, Harrigan P, Heineike B, Stewart-Ornstein J, El-Samad H. Building robust functionality in synthetic circuits using engineered feedback regulation. Curr Opin Biotechnol. 2013; 24:790–796. [PubMed: 23566378]

98. Perrimon N, Barkai N. The era of systems developmental biology. Curr Opin Genet Develop. 2011; 21:681–683.

99. Landau, LD.; Lifshitz, EM. Course of theoretical physics volume 6: Fluid mehcanics. Butterworth-Heinemann; 1987.

100. Francis K, Palsson BO. Effective intercellular communication distances are determined by the relative time constants for cyto/chemokine secretion and diffusion. Proc Natl Acad Sci U S A. 1997; 94:12258–12262. [PubMed: 9356436]

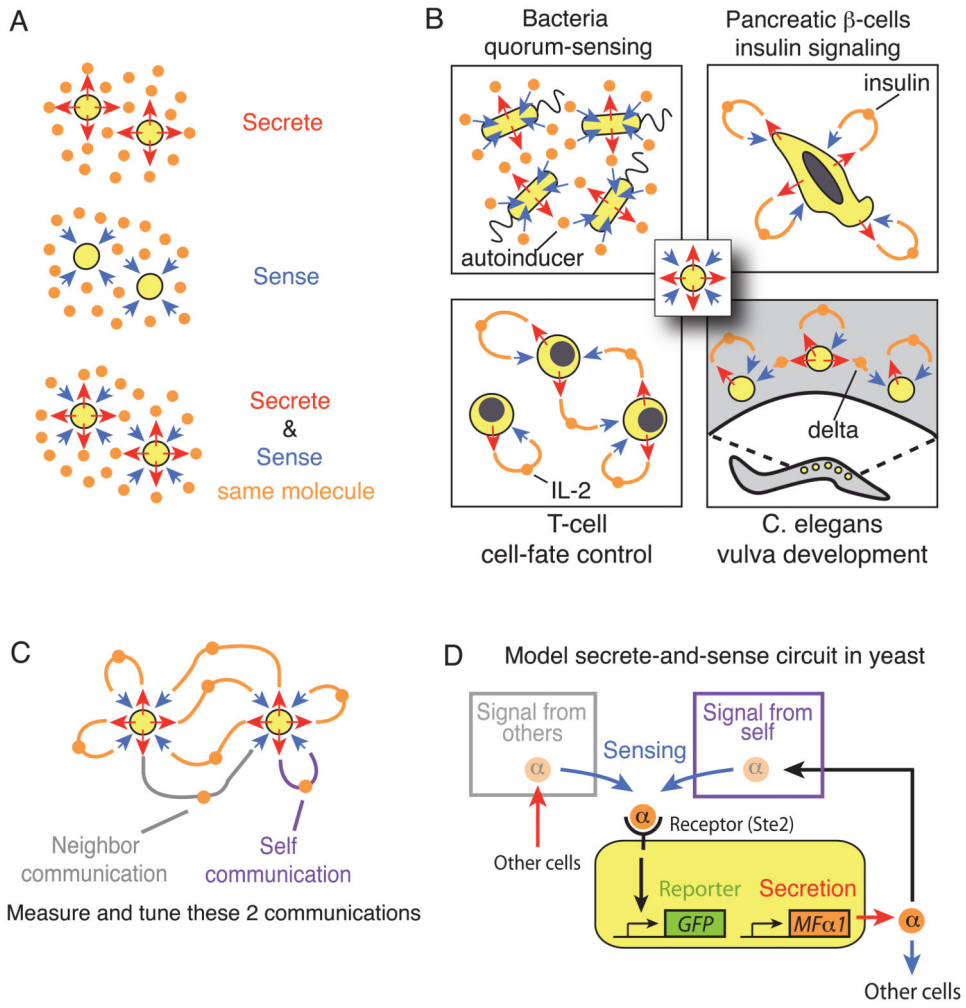

Fig. 1. Synthetic secrete-and-sense circuit motif in yeast

(A) Cells that secrete a signaling molecule without sensing (top), cells that sense a molecule without secreting (middle), and cells that secrete and sense the same signaling molecule (bottom). **(B)** Examples of 'secrete-and-sense' cells in nature: bacteria secrete and sense an autoinducer for sensing a quorum, human pancreatic beta-cells secrete and sense insulin, human T cells secrete and sense the cytokine interleukin-2 to control their proliferation, and the vulva precursor cells in *C. elegans* secrete and sense the diffusible Delta for specifying their cell-fates. **(C)** Schematic of self-communication and neighbor-communication between two identical secrete-and-sense cells. **(D)** Schematic of synthetic secrete-and-sense system: haploid budding yeast (yellow box) engineered to secrete and sense α-factor (orange circle). GFP fluorescence is a read-out of the concentration of α-factor sensed by the cell.

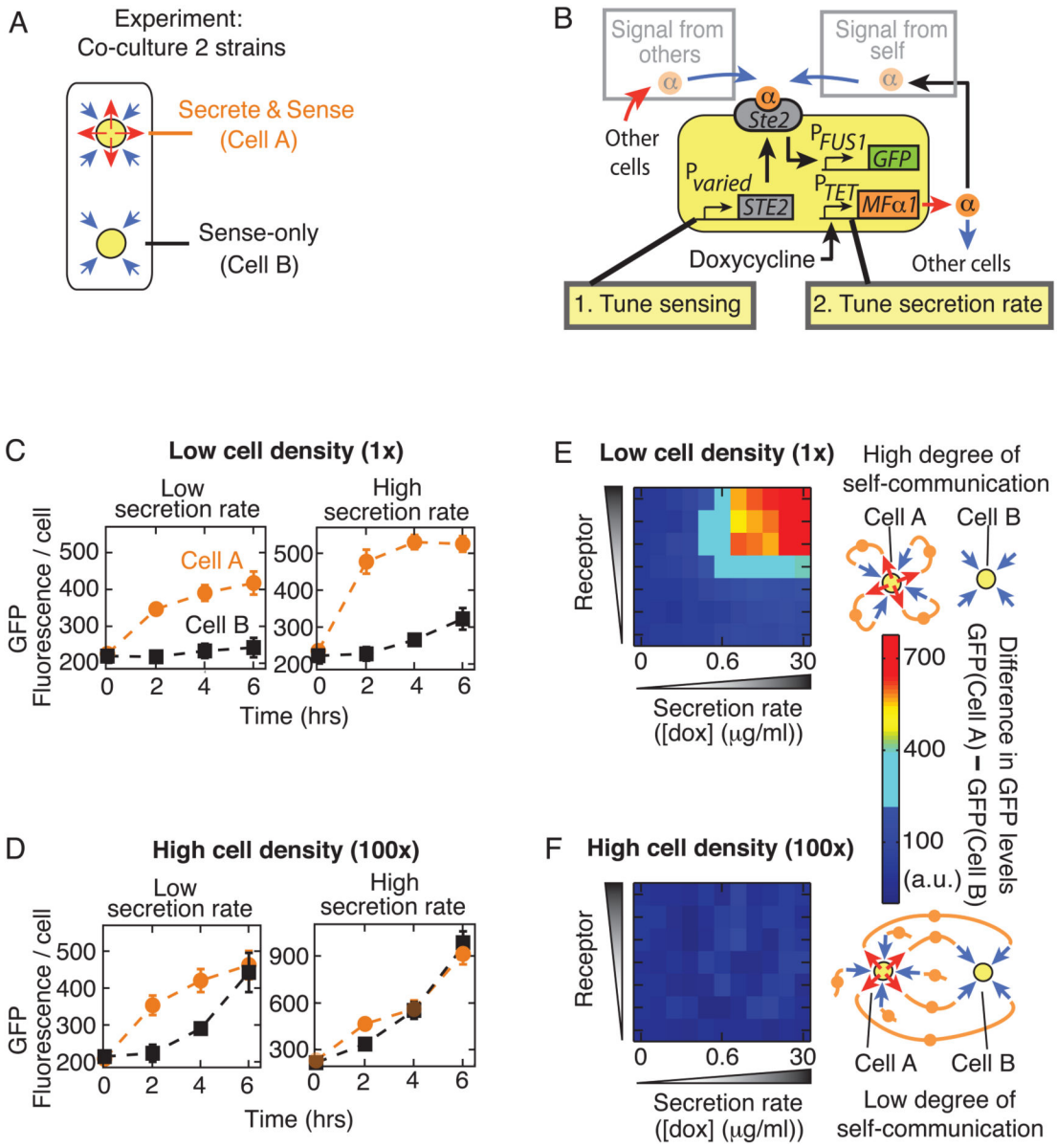

Fig. 2. Varying receptor abundance and secretion rate to tune degrees of self- and neighbor-communication

(A) Secrete-and-sense strain (‘Cell A’) and sense-only strain (‘Cell B’) were cultured together for all experiments in this figure. **(B)** Each secrete-and-sense strain used a different promoter P_{varied} to express *STE2* but all used the *pTET07* to express *MFα1*. For each secrete-and-sense strain, a matching sense-only strain with the same Ste2 abundance was constructed. **(C-D)** Equal densities of ‘basic secrete-and-sense strain’ and ‘basic sense-only strain’ were cultured together for two representative doxycycline concentrations: [doxycycline] = 6 μg/ml (‘low secretion rate’) and 30 μg/ml (‘high secretion rate’), and at two total cell densities: (C) low (OD = 0.001) and (D) high (OD = 0.1). Each strain's single-cell GFP fluorescence at various time points are shown. Error bars: SEM, *N*=3. **(E-F)** Each secrete-and-sense strain (‘Cell A’) was cultured with its partner sense-only strain (‘Cell B’) (i.e., Ste2 expressed by the same promoter in both strains). 7 such pairs of strains were

cultured for five hours in 11 different concentrations of doxycycline (table S1, fig. S8), yielding heat maps with 7×11 pixels for (E) low (OD=0.001) and (F) high (OD=0.1) cell densities. Each pixel represents the difference between the GFP fluorescence of Cell A and of Cell B at the end of the time course (subtracting GFP fluorescence of Cell B from that of Cell A, averaged from three independent experiments).

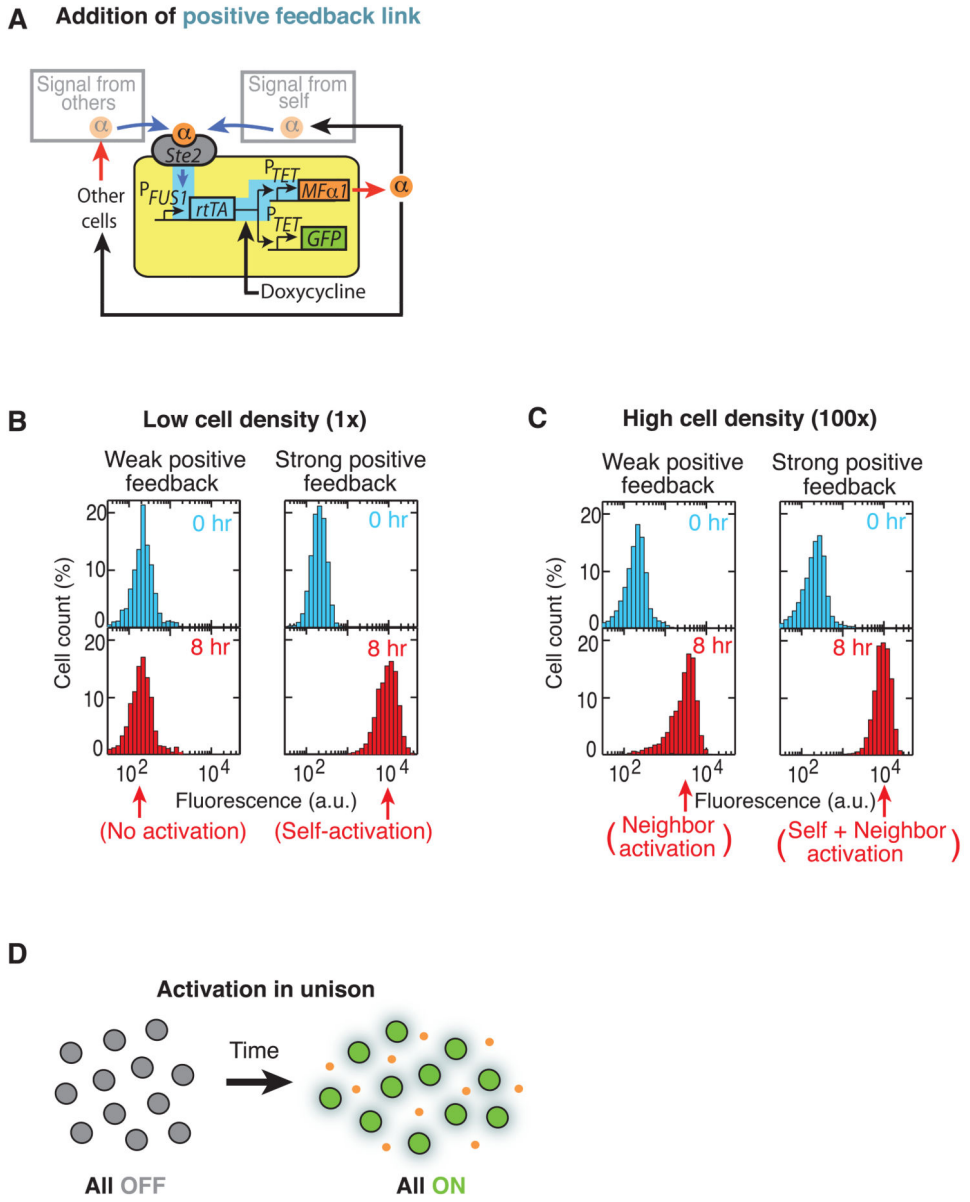

Fig. 3. Effects of self- and neighbor-communication on positive feedback linking secretion with sensing

(A) Basic secrete-and-sense circuit modified by a positive feedback link (highlighted in blue). **(B-C)** Representative histograms showing the single-cell GFP fluorescence level of the basic secrete-and-sense strain with the positive feedback link obtained by a flow cytometer. This strain was cultured by itself at two different initial cell densities ((B) low cell density (OD=0.001), (C) high cell density (OD=0.1)) and in two representative concentrations of doxycycline ([doxycycline] = 3 μg/ml: weak positive feedback, and [doxycycline] = 40 μg/ml: strong positive feedback). Blue histograms: beginning of the time-course (0 hour) and red histograms (8 hours into the time course) (full data sets in figs. S11 and S12). Under each panel, the corresponding type of activation behavior is mentioned. **(D)** Main population-level behavior: Activation of all cells in near unison.

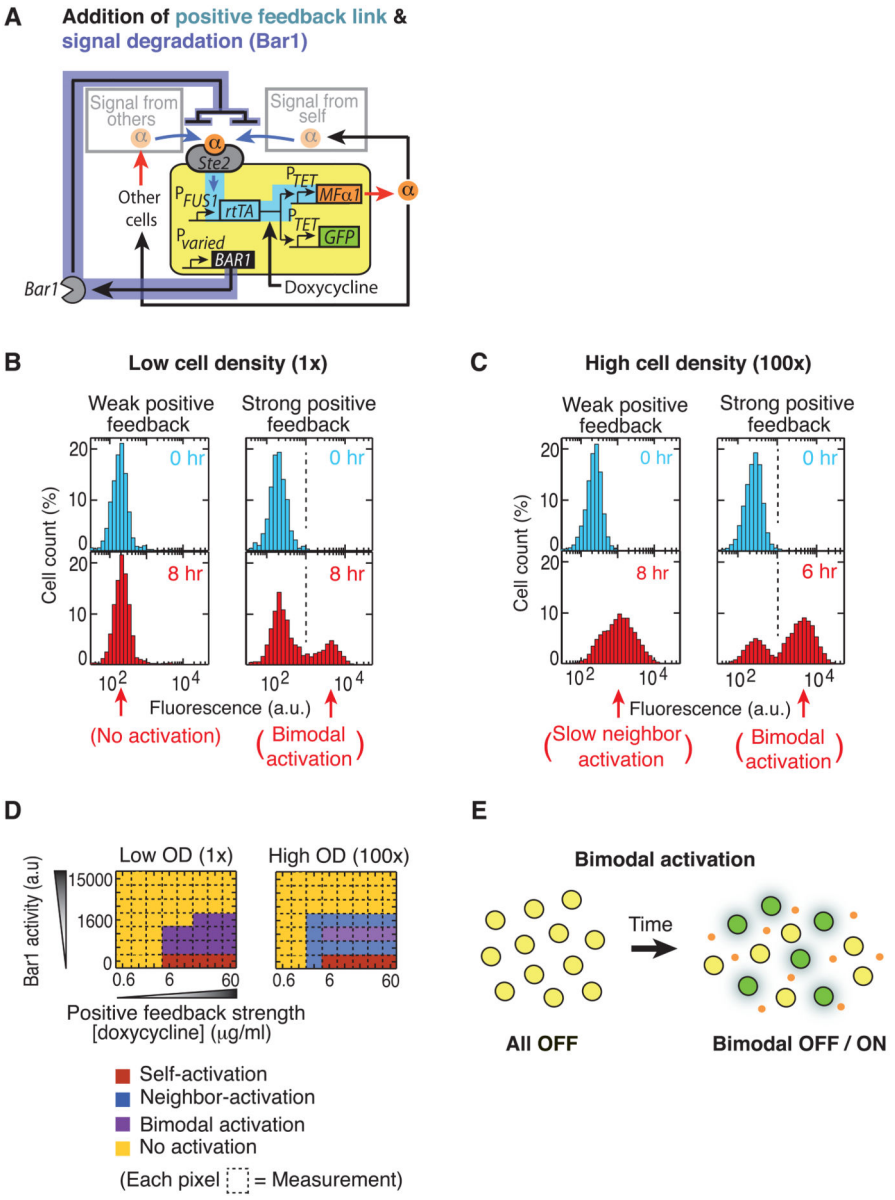

Fig. 4. Effects of self- and neighbor-communication on positive feedback with signal degradation

(A) Basic secrete-and-sense circuit with positive feedback link (blue highlight) and the Bar1 protease (grey). Six different strains of this type were constructed, each with a different constitutive promoter P_{varied} controlling expression of *BAR1*. **(B-C)** An example strain (with *pCYC1-BAR1*) cultured by itself at two different initial cell densities ((E) low cell density (OD=0.001), (F) high cell density (OD=0.1) and in two representative doxycycline concentrations ([doxycycline]= 6 μg/ml (weak positive feedback), and 20 μg/ml (strong positive feedback)). Representative histograms showing the single-cell GFP fluorescence levels of this strain are plotted at two different time points (blue and red histograms). Under each panel, the corresponding type of activation behavior is mentioned (figs. S14 and S15). **(D)** Phase diagrams from analyzing each time-course for the seven secrete-and-sense strains, each with different amounts of Bar1 (including none, Fig. 3) and positive feedback strengths

at low (OD=0.001) and high (OD=0.1) cell density cultures (summarizes fig. S11, S12, S14, and S15). **(E)** Main population-level behavior: Bifurcation of an isogenic population into subpopulations of quiescent and maximally secreting cells.

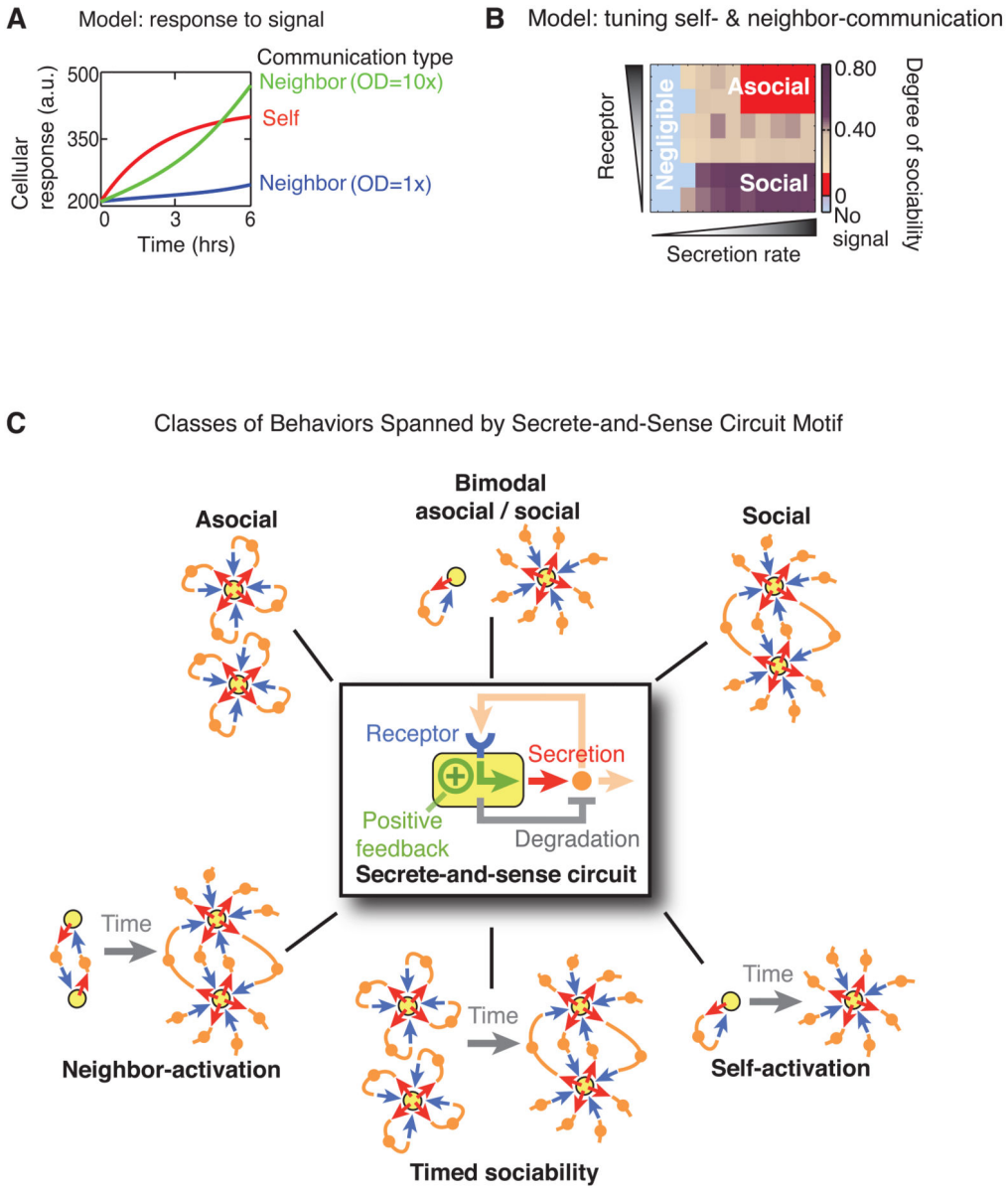

Fig. 5. A simple mathematical model provides intuition

(A-B) A phenomenological model provides qualitative insights underlying the main features of the secrete-and-sense circuit revealed by our experiments (61). (A) Model explains the individual cellular response of a secrete-and-sense cell that self-communicates (red curve) and of a sense-only cell at a low cell density (blue curve) and at a higher cell density (green curve). These curves are analogous to those seen in Fig. 2, C and D. (B) Model summarizes self- and neighbor-communication in a phase diagram representing the 'degree of sociability' (defined in Supplementary Text (61)). **(C)** Summary of the main behavioral classes spanned by the secrete-and-sense circuit motif.

Table 1

Design table for engineering secrete-and-sense cells with desired biological functions motivated by our synthetic secrete-and-sense circuit

Examples of biological functions of secrete-and-sense cells that can be understood and engineered based on the design principles revealed by our synthetic circuit.

Desired biological function	Possible circuit parameters for realizing desired biological function	Mode of communication used (Neighbor / Self)	Class of behavior (Fig. 5C)
Quorum sensing	• Low receptorabundance • Weak positivefeedback	Neighbor	• Purely social
Monoclonal expansion of cells in a polyclonal culture due to sensing of self-secreted cytokines	• High receptor abundance and high secretion rate • Strong positive feedback	Self	• Purely asocial • Self-activation • Timed-activation
Creating two functionally distinct cell states	• Moderate to strong positive feedback	Self and neighbor	• Self-activation • Neighbor-activation • Timed-activation
Differentiating an isogenic population into two populations of functionally distinct cells that coexist with a defined ratio	• Moderate positive feedback with low signal degradation • Strong positive feedback with moderate signal degradation	Self and neighbor	• Bimodal activation • Self-activation • Neighbor-activation • Timed-activation